Hindawi Publishing Corporation
International Journal of Antennas and Propagation
Volume 2012, Article ID 895390, 13 pages
doi:10.1155/2012/895390

Research Article

Unambiguous Multipath Mitigation Technique for BOC(*n*,*n*) and MBOC-Modulated GNSS Signals

Khaled Rouabah,[1] Mustapha Flissi,[1] Salim Attia,[1] and Djamel Chikouche[2]

[1] *LMSE Laboratory, Electronics Department, University of Mohamed Bachir El-Ibrahimi, Elanasser, Bordj Bou Arréridj 34265, Algeria*
[2] *LASS Laboratory, Electronics Department, University of M'sila, M'sila 28000, Algeria*

Correspondence should be addressed to Khaled Rouabah, khaled_rouabah@yahoo.fr

Received 15 March 2012; Revised 28 June 2012; Accepted 2 July 2012

Academic Editor: Athanasios Panagopoulos

We propose an efficient scheme for side peaks cancelation and multipath (MP) mitigation in binary offset carrier (n,n) (BOC(n,n)) and multiplexed BOC (MBOC) modulated signals. The proposed scheme reduces significantly the band of variation of MP errors in global navigation satellite system (GNSS). It consists of two versions. The first one is based on the use of maximum likelihood estimator (MLE) of MP signals and reference correlation functions (CFs) like that of pseudorandom noise (PRN) code without BOC subcarrier. In the second version, the former (MLE) is used with the reference BOC(n,n) or MBOC CFs. Unlike traditional BOC(n,n) and MBOC, that have CFs containing multiple peaks leading to potential tracking ambiguities, our proposed scheme does not contain any side peaks. In addition, all the MP signals with medium and long delays have no effect on the estimation of the pseudorange. On the other hand, all the methods proposed for mitigating MP in no-BOC scheme are practical for our scheme due to its CF which is similar to that of the PRN code. The computer simulation results show that the proposed scheme has superior performances in the reduction of the errors produced in the process of the delay estimation of line of sight (LOS) and caused by MP propagation. In fact, the performances of the proposed scheme are better with regard to that of the traditional BOC(n,n) and MBOC. Moreover, in the presence of noise, our proposed scheme keeps better performances than the common side peaks cancelation methods.

1. Introduction

GNSS like global positioning system (GPS) and future Galileo [1] utilizes BOC [2] and MBOC [3] modulations for improving tracking performances and for MP mitigation. MBOC spreading modulation has been recommended by the GPS-GALILEO Working Group on Interoperability and Compatibility [4]. However, positioning accuracy is seriously degraded due to the presence of side peaks in CFs which present ambiguous tracking [5, 6]. The BOC(m,n) modulations are expected to enable better receiver tracking performance compared to BOC(1,1) and MBOC schemes. Yet, it has been found out that the tracking loop design for BOC(m,n) may be more problematic than for BOC(1,1) and MBOC, especially with the conventional delay locked loop (DLL) algorithm with narrow correlator (NC) [7]. In contrast to the BOC(n,n) modulation, the BOC(m,n) "$m \neq n$" CFs produce several side peaks which complicate the DLL-locking operation. Various techniques are proposed for side peaks cancelation. The most basic of them are built on the basis of the CF of the BOC(m,n) and MBOC signals. Thus, in [8], a method of combining the CF of the received signal and a reference BOC-PRN, one has been proposed for side peaks cancelation in BOC-modulated signals. In the ideal case, the method gives the better performances. However, side peaks still exist in the resulting CF in the presence of MP signals. In [9], the authors have proposed a side peaks cancelation method (SCM) based on the construction of a reference BOC-PRN CF by estimating the channel response. The constructed BOC-PRN reference CF is then used to reduce the effect of side peaks in the CF of the received signal. The method has some degree of

optimization. However, some side peaks are always present in the resulting CFs because there are differences between the slopes of the CF of the received signal and the BOC-PRN reference CF. In [10], the authors have proposed a method based on the combination of the CF of the received signal and its absolute value. The method is labeled absolute autocorrelation function (AACF) method. This method is shown to give better performances in some situations and it is limited in others especially when the MP signal is in 180° (out of phase with respect to the LOS). Other techniques based on the modification of the locally generated codes are proposed in literature. For example, in [11], the authors have proposed new waveforms of locally generated codes. Therefore, the CF is calculated between the received signal and these new waveforms and it is called pseudo-CF (PCF). As a consequence, in ideal situations, the method gives better performances. However, the method is limited by the presence of MP and noise because it consists of blanking a significant part of the received signal. In addition, the resulting CF is completely deformed which is another limitation. In [12], the authors have proposed a method based on the computation of the BOC-PRN CF instead of the BOC-BOC one. The method is simple for implementation and has shown to completely eliminate side peaks in the CF of the received signal. Besides, the method does not require the use of a DLL loop. However, the method is limited by the MP. In fact the performances of this method are similar to those of the wide correlator in the traditional CF of the Coarse/Acquisition (C/A) code. In [13], the authors have extended the BOC-PRN method to MBOC modulated signal. The performances of this latter are similar to the original version and it presents the same limitations. In [14], the authors have added improvements to the aforementioned method in the presence of MPs. The result is a narrow unambiguous discriminator within the receiver operational range of $(-1,1)$ chip, which appears like that of the high-resolution correlator (HRC) and strobe correlator (SC) [15–17] for a PSK signal. Contrary to the HRC and SC, this method is limited by the early late spacing between the correlators which can take only one value. In fact, another value of early late spacing will generate ambiguous points [14]. This last method can be used in conjunction with the enhanced HRC [18] to improve the performances.

To sum up, the given different methods have different limitations. Some methods are sensitive to the MPs with long delay (Between 0.5 and 1 chip). Other methods are only valid in the case of the absence of MP signals and they have not been tested in the MP environments where, as we are going to see it later, the performances are completely degraded. The rest of the methods give a weak elimination of the side peaks. Consequently, the ambiguity in the CF is always present and there is an influence of the MP on these methods.

In this paper, we propose an efficient method to completely eliminate the side peaks in the BOC(n,n) and MBOC modulations (like composite BOC (CBOC) and time-multiplexed BOC (TMBOC)). The proposed scheme is shown to have a medium complexity compared to the most effective methods. On the other hand, due to the complete absence of the side peaks in the CF, all the methods used for MP mitigation in no-BOC signals such as HRC [15], SC [17], multipath estimating DLL (MEDLL) [19, 20], multipath estimating technologie (MET) [21], fast iterative maximum-likelihood algorithm (FIMLA) [22], and the virtual MP mitigation technique (VMMT) [23–25], among others, are practical for our proposed scheme and, thus, the use of these techniques in combination with our proposed scheme gives a better performance in the presence of MP signals. Finally, our proposed scheme presents a better resistance to the MP and the precorrelation bandwidth in the receiver compared to the traditional CF (like BOC(n,n) and MBOC) due to the reduced width of its CF.

Because the BOC(n,n) CF has the same form for all the values of n, we discuss only the case of BOC(1,1) CF ($n = 1$). With the same discussion, we can generalise the method for case with any value of "n."

The paper is organised as follows: we begin with a description of the BOC and MBOC modulation schemes and the principle of our proposed scheme. After that, we carry a comparison between the BOC, MBOC schemes, and ours. Later on, we present the comparison between the combination of our scheme with HRC and the combination of traditional BOC and MBOC schemes with HRC. Finally, we end up by the performances comparison between the proposed scheme and the common side peaks cancelation schemes.

2. BOC and MBOC Modulations

BOC is a square waveform subcarrier modulation, where a signal $s(t)$, the signal which is going to be modulated, is multiplied by a square waveform subcarrier of frequency f_{sc}. Formally, the BOC-modulated signal $s_{BOC}(t)$ can be written as [1, 2]:

$$s_{BOC}(t) = s(t) \cdot \operatorname{sign}\left(\sin\left(2\pi f_{sc} t\right)\right). \tag{1}$$

For Galileo signals, the notation BOC(m,n) is used, where m and n are two indices satisfying the relationships:

$$\begin{aligned} m &= \frac{f_{sc}\,[\text{MHz}]}{1.023\,[\text{MHz}]}, \\ n &= \frac{f_X\,[\text{MHz}]}{1.023\,[\text{MHz}]}, \end{aligned} \tag{2}$$

where f_X is the chiprate of the PRN code and 1.023 [MHz] is the chiprate of C/A GPS code.

We remark that the subcarrier frequency and the chiprate are always integer multiples of 1.023 MHz frequency [2]. BOC(1,1) modulation generalizes one zero crossing on spreading code chip. The number of zero crossing in one chip of the PRN code is proportional to both subcarrier frequency and chiprate code. An example showing the BOC-modulated waveform is given in Figure 1 for BOC(1,1) modulation.

In this figure, the waveform of the subcarrier, the spreading code and the resulting modulated BOC signal are plotted. The CFs of both no-BOC and BOC(1,1) modulated signals are shown in Figure 2.

As illustrated in this figure, each of these CFs presents an advantage and an inconvenience. Indeed, the no-BOC

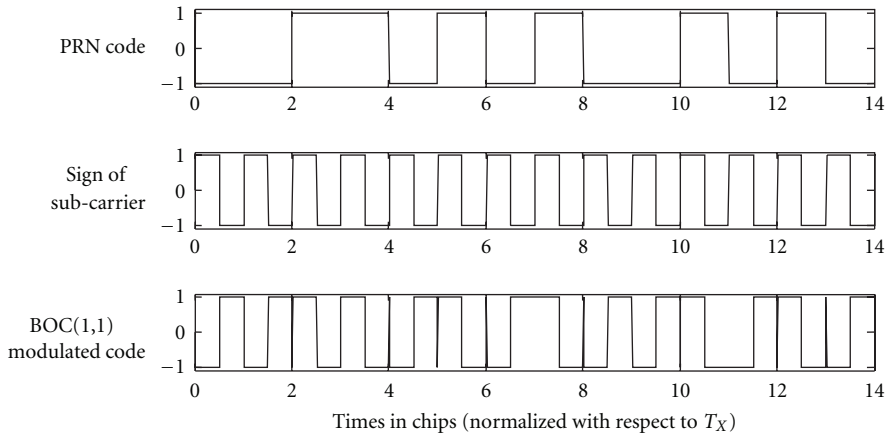

Figure 1: BOC(1,1) modulation.

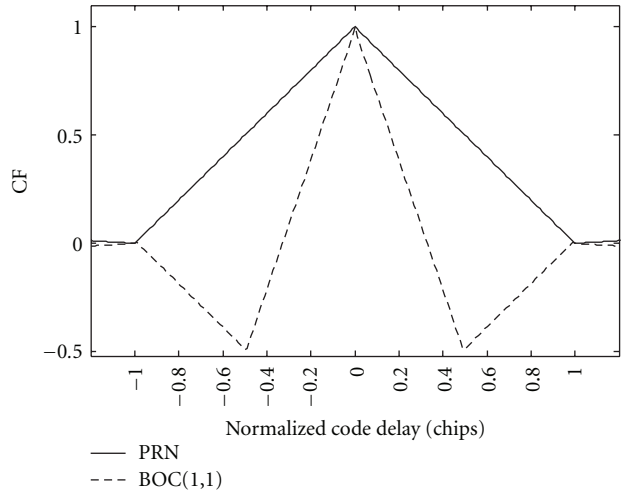

Figure 2: Normalized CFs for both PRN and BOC(1,1) codes.

CF (PRN CF) presents the inconvenience of the large width (which degrades the performances in presence of MP) and the advantage of the absence of the side peaks (which eliminates ambiguity). In contrast to the no-BOC-modulated signal, the BOC(1,1) one presents the advantage to have a sharpest CF and the inconvenience of the presence of the side peaks that can create an ambiguity in the operation of tracking.

Another type of modulation has been proposed to improve the code tracking performance. This type is about MBOC and is defined in the frequency domain. Its power spectral density (PSD) is the combination of both BOC(1,1) and BOC(6,1) PSDs according to the following equation:

$$G_{\mathrm{MBOC}}(f) = \frac{10}{11} G_{\mathrm{BOC}(1,1)}(f) + \frac{1}{11} G_{\mathrm{BOC}(6,1)}(f), \quad (3)$$

where $G_{\mathrm{BOC}(1,1)}(f)$ is the PSD of BOC(1,1) code, $G_{\mathrm{BOC}(6,1)}(f)$ is the PSD of BOC(6,1) code, and $G_{\mathrm{MBOC}}(f)$ is the PSD of MBOC code.

It is often noted MBOC(6,1,1/11), where the term (6,1) refers to the BOC(6,1) modulation, and the ratio of 1/11 represents the distribution of the power between the constituents of BOC(1,1) and BOC(6,1) PSDs. The contribution of the BOC(6,1) subcarrier brings a more important quantity of energy on high frequencies than the BOC(1,1) subcarrier that leads to a signal with sharper CF and thus gives the best performances in positioning the receiver [3, 4].

In TMBOC implementation, the whole signal is divided into blocks of N code symbols [26]. Out of the N code symbols, $M < N$ symbols are BOC(1,1) modulated and the remaining $N - M$ code symbols are BOC(6,1) modulated [26].

The forms of the CFs of no-BOC, CBOC(1,6,10/11), and TMBOC(1,6,10/11) are shown in Figure 3.

From this figure, it can be observed that the main peaks of CBOC and TMBOC are narrower than that of no-BOC which improves the performances. However, unlike no-BOC CF, CBOC and TMBOC CFs present side peaks.

3. Principle of the Proposed Side Peaks Cancelation Method

3.1. Ideal Case. To overcome the limitation of BOC(1,1), CBOC, and TMBOC modulations, in term of side peaks influence, we propose a combination of these traditional CFs with reference CFs of PRN code (CF of no-BOC). The principle of BOC(1,1) side peaks cancellation is illustrated in Figure 4.

As shown in this figure, the line segments of no-BOC (Solid green line) and BOC(1,1) (Dashed red line) CFs have the same slopes with opposite signs in the intervals of $[-1,-0.5]$ and $[0.5,1]$ with respect to the chip delay. In effect, the sum of these two CFs, in these intervals, gives zero. By this combination, we reduce significantly the width of the main peak as shown in the latter figure (solid red line). Consequently, different to the no-BOC and BOC(1,1) CFs that have a width of two chips in the horizontal axis, the resultant CF of our proposed combination has a width of only one chip on the horizontal axis (Solid red line). This advantage gives to the proposed method a

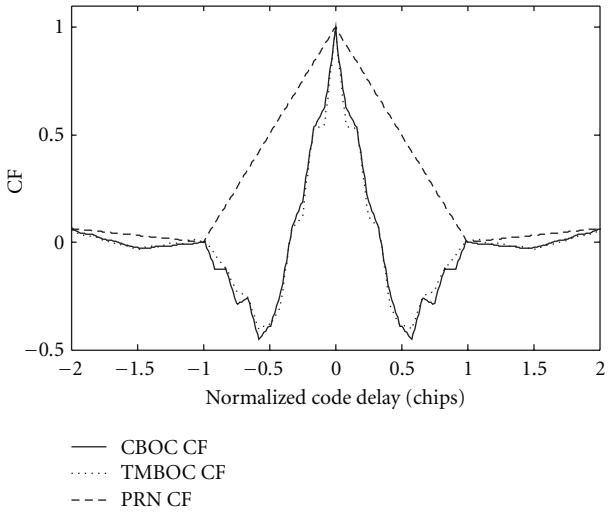

Figure 3: Normalized CFs for PRN, CBOC, and TMBOC codes.

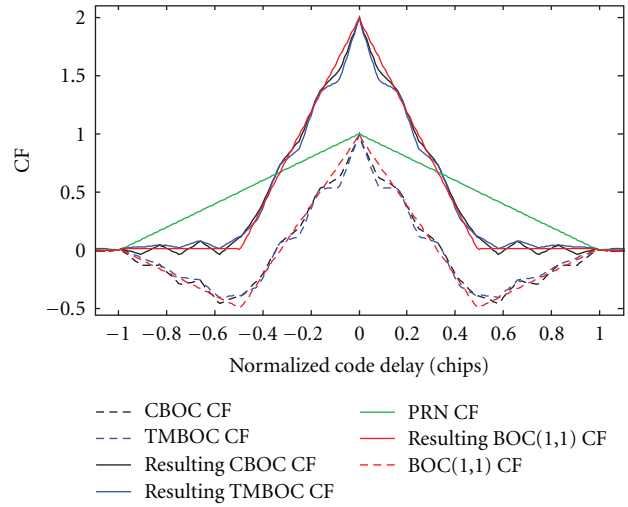

Figure 4: Normalized CFs for PRN, CBOC, and TMBOC codes and the resultants CFs after the application of the proposed method (1st version).

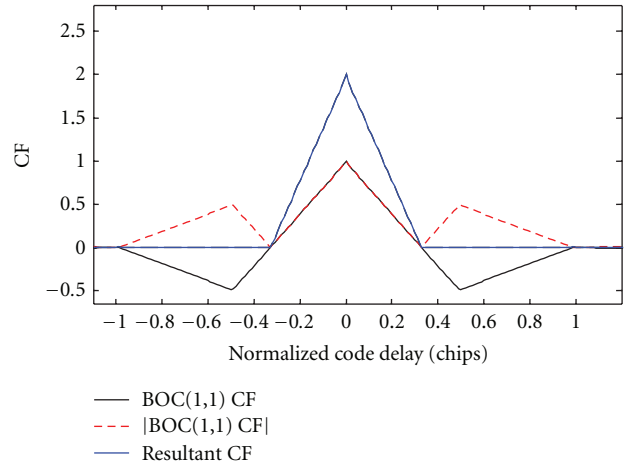

Figure 5: Normalized CF of BOC(1,1), absolute CF of BOC(1,1), and the resultant CF after application of the proposed method (2nd version).

better performance than that of both BOC(1,1) and no-BOC signals as we are going to see in the last part of this paper.

Similarly to the BOC(1,1) modulation, the side peaks cancelation of TMBOC (dashed blue line) and CBOC (dashed black line) are obtained by the same principle. Here, we cannot eliminate the side peaks but we can completely reduce their amplitudes. The principles of both CBOC and TMBOC side peaks cancelation methods are illustrated in Figure 4. The widths of the resultant CFs of both CBOC and TMBOC (solid blue and solid black lines) are divided to approximately half in comparison to the traditional ones. The principle of using the PRN reference CF is the first version of our proposed scheme. We can have better performances while combining the absolute of reference CFs not of PRN codes but of, respectively, BOC(1,1), CBOC, and TMBOC codes. This is the second version of the proposed scheme and the principle is shown in Figures 5, 6, and 7, respectively, for BOC(1,1), CBOC, and TMBOC codes.

As illustrated in these figures, the side peaks of BOC(1,1), CBOC, and TMBOC are completely eliminated compared to the resulting CFs obtained by the application of the first version of the proposed scheme which present very weak side peaks especially in CBOC and TMBOC CFs.

To summarize, as shown in Figure 8, the difference between the first and the second versions is in the fact that in the first version the segments of BOC(1,1) and no-BOC CFs (solid red line and solid brown line) have the same slopes with opposite signs in the intervals of $[-1,-0.5]$ and $[0.5,1]$ with respect to the chip delay.

On the contrary, in the second version, the segments of the BOC(1,1) CF and the absolute reference one have the same slopes with opposite signs in the intervals $[-1,-0.33]$ and $[0.33,1]$ with respect to the chip delay (dashed black line and solid brown line). Hence, the widths of the CFs of all codes, obtained with the second version, are reduced in comparison to what we observe in CFs of all codes, obtained with the first version. The widths of the CFs resulting from the first and the second versions are, respectively, 1 and 2/3 with respect to the chip delay. This has a great impact on the performances as we are going also to see in the last part of this paper.

The discussions in this section of paper are only focused on a positive CF. This case is valid when the cosine of the phase of the received signal is positive. However, as for the negative CF, once detected, based on the estimation of the phase of the received signal, it can be treated by multiplying the reference CF, used for side peaks cancellation, by the cosine of the phase of the received signal.

In the following section of this paper, we shall describe the principle of estimating the phase of the received signal which can take 0° (in phase) or (180°) out of phase or other values.

Both PRN CF and the absolute BOC CF are reference functions that are generated one and stored in memory.

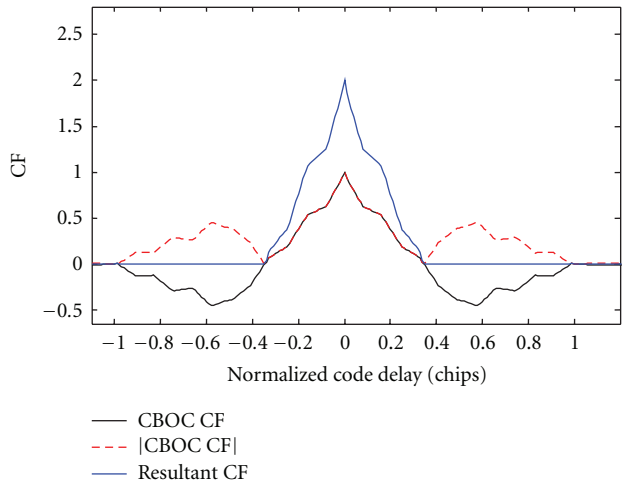

Figure 6: Normalized CF of CBOC, absolute CF of CBOC, and the resultant CF after application of the proposed method (2nd version).

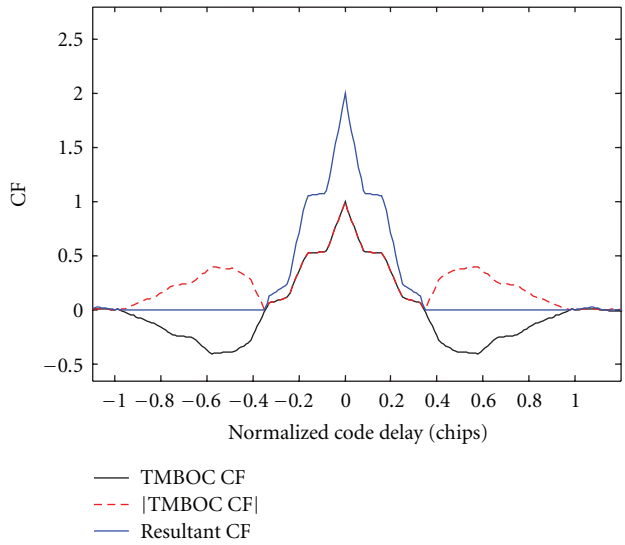

Figure 7: Normalized CF of TMBOC, absolute CF of TMBOC, and the resultant CF after application of the proposed method (2nd version).

In the receiver side, they are extracted from the memory and combined with the ambiguous CF, after a phase of alignment, to perform side peaks cancelation. Consequently, our method provides less time-consuming and simpler approach.

In order to obtain an unambiguous CF shape, the reference PRN CF (resp. the absolute value of the BOC CF) has to be subtracted from the ambiguous CF of the received signal as follows:

$$R_{\text{Unambiguous}V1}(\tau) = R_{\text{Ambiguous}}(\tau) + \hat{a}\cos\left(\hat{\theta}\right)R_{\text{Ideal-PRN}}(\tau),$$

$$R_{\text{Unambiguous}V2}(\tau) = R_{\text{Ambiguous}}(\tau) + \hat{a}\cos\left(\hat{\theta}\right)\left|R_{\text{Ideal-BOC}}(\tau)\right| \quad (4)$$

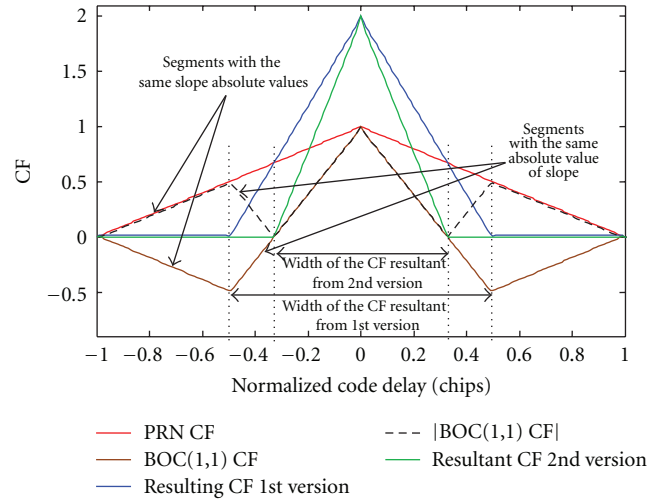

Figure 8: Difference between the 1st and the 2nd versions in term of width of the resultant CF.

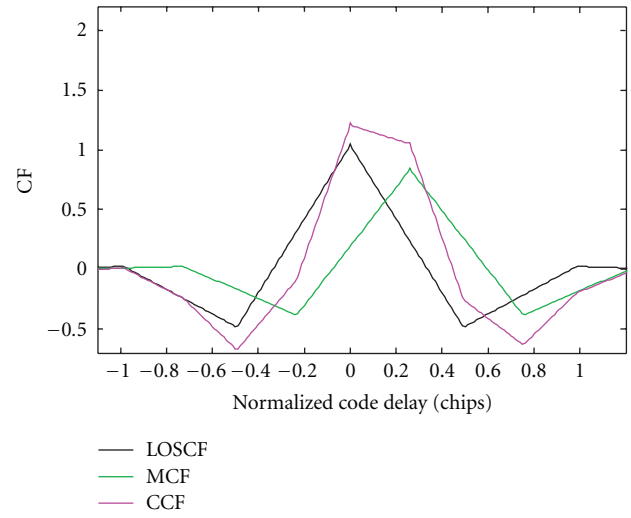

Figure 9: LOSCF, MCF, and CCF.

with $\hat{a}$: the estimated amplitude of the received signal, $\hat{\theta}$: the estimated phase of the received signal, $R_{\text{Unambiguous}V1}(\tau)$: the desired unambiguous CF (1st version), $R_{\text{Unambiguous}V2}(\tau)$: the desired unambiguous CF (2nd version), $R_{\text{Ambiguous}}(\tau)$: the CF of the received signal, $R_{\text{Ambiguous}}(\tau)$: the CF of the received signal, $R_{\text{Ideal-PRN}}(\tau)$: the ideal reference PRN CF, and $R_{\text{Ideal-BOC}}(\tau)$: the ideal reference BOC CF.

3.2. Influence of MP Signals. In the presence MP propagation, the received signal at the input of the a receiver can be written as follows [21]:

$$S_r(t) = \sum_{i=0}^{M} a_i p(t-\tau_i)\cos(wt+\theta_i) + n(t) \quad (5)$$

with a_i: the amplitude of ith MP component, τ_i: the delay of ith MP component ($i \neq 0$), θ_i: the phase of ith MP component ($i \neq 0$), a_0: the amplitude of LOS component

($i \neq 0$), τ_0: the delay of LOS component, θ_0: the phase of LOS component, $n(t)$: the white Gaussian noise, and $p(t)$: the PRN code modulated with the subcarrier.

In the presence of LOS and a single MP signal, the receiver tries to correlate with these two components. The CF of the received signal is distorted as shown in Figure 9 for BOC(1,1) code (solid magenta line).

Analytically, the LOS and MP signals may be treated separately. Thus, we may consider the CF associated with LOS (LOSCF, solid black line) and the CF associated with MP signal (MCF, solid green line). At any point, these two CFs can be vector summed to yield the CF associated with the composite signal (CCF, solid magenta line).

In reality, the direct application of the proposed method to the CCF of the received signal does not perfectly eliminate side peaks. This is one limitation of several side peaks cancelation methods. These side peaks are function of the parameters of MP and LOS signals (Delays, amplitudes and phases). Even in the presence of two components or more, some side peaks may always occur which leads to the ambiguity on the operation of tracking.

To solve this problem, several reference CFs must be combined to be used for side peaks cancelation. Indeed, for each component of the received signal, a reference CF is necessary for side peaks cancelation of the corresponding CF. In fact, all the components of the received signal should be estimated. We should thus estimate the amplitudes, the delays and the phases of all the components of the received signal. Several techniques can be used for this. Among these techniques, one can quote: reference correlation MP mitigation (RCMPM) [23], FIMLA [22], MEDLL [19, 20], and MMT [21]. All these techniques use statistics to estimate the parameters of all the components of the received signal. In this paper, we use the technique MEDLL. The practical receiver implementation of this technique requires the measurement of the CCF of the received signal in order to detect the shape and the distortions caused by all the components of the received signal. The CCF can be sampled via using a bank of correlators [23]. The samples of the CCF of both no-BOC and BOC(1,1), obtained by using the bank of correlators are shown in Figure 10.

We use a number of correlators (N) distributed across the received CCF. According to MLE, the MEDLL calculates the estimates which minimize the mean square error, between the received and the estimated signals, given by

$$L\left(\hat{a}, \hat{\tau}, \hat{\theta}\right) = \int_{t-T}^{t} [S_r(t) - S(t)]^2 dt, \tag{6}$$

where $S(t)$ is the estimate of the LOS plus multipath signals. It is given as

$$S(t) = \sum_{i=0}^{M} \hat{a}_i p(t - \hat{\tau}_i) \cos\left(wt + \hat{\theta}_i\right) \tag{7}$$

with $\hat{a}_i$: the estimated amplitude of ith MP component ($i \neq 0$), $\hat{\tau}_i$: the estimated delay of ith MP component ($i \neq 0$), $\hat{\theta}_i$: the estimated phase of ith MP component ($i \neq 0$), $\hat{a}_0$: the estimated amplitude of LOS component, $\hat{\tau}_0$: the estimated delay of LOS component, and $\hat{\theta}_0$: the estimated phase of LOS component.

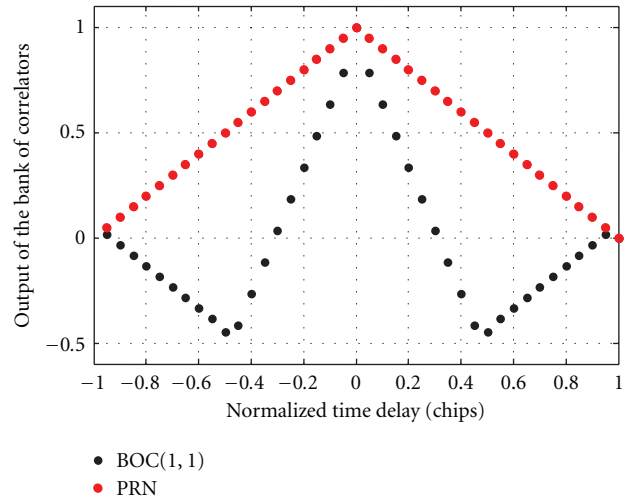

Figure 10: Multiple correlator sampling of the CF.

These estimates can be given, from (6), as follows [19]:

$$\hat{\tau}_m = \max_{\tau} \left\{ \mathrm{Re}\left[\left(R_x(\tau) - \sum_{\substack{i=0 \\ i \neq m}}^{M} \hat{a}_i R(\hat{\tau} - \hat{\tau}_i) \exp\left(j\hat{\theta}_i\right) \right) \times \exp\left(-j\hat{\theta}_m\right) \right] \right\}, \tag{8}$$

$$\hat{a}_m = \mathrm{Re}\left[\left(R_x(\hat{\tau}_m) - \sum_{\substack{i=0 \\ i \neq m}}^{M} \hat{a}_i R(\hat{\tau}_m - \hat{\tau}_i) \exp j\left(\hat{\theta}_i\right) \right) \times \exp\left(-j\hat{\theta}_m\right) \right], \tag{9}$$

$$\hat{\theta}_m = \arg\left[R_x(\hat{\tau}_m) - \sum_{\substack{i=0 \\ i \neq m}}^{M} \hat{a}_i R(\hat{\tau}_m - \hat{\tau}_i) \exp\left(j\hat{\theta}_i\right) \right], \tag{10}$$

$$R_x(\tau) = \frac{1}{T} \int_{t-T}^{t} \tilde{S}_r(t) p(t - \tau) \exp(-jW_i t) dt, \tag{11}$$

$$R(\tau) = \frac{1}{T} \int_{t-T}^{t} p(t) p(t - \tau) dt \tag{12}$$

with $R_x(\tau)$: the samples of CCF of the received signal, $R(\tau)$: the reference CF, and M: the number of MP signals.

The estimation of phase from (10) characterizes the coherent configuration. In the noncoherent configuration, the phase information is lost due to noncoherent integration, thus this is recovered by generating random (uniformly distributed in [0 2π]) phases and by choosing that one corresponding to the minimum mean-square error.

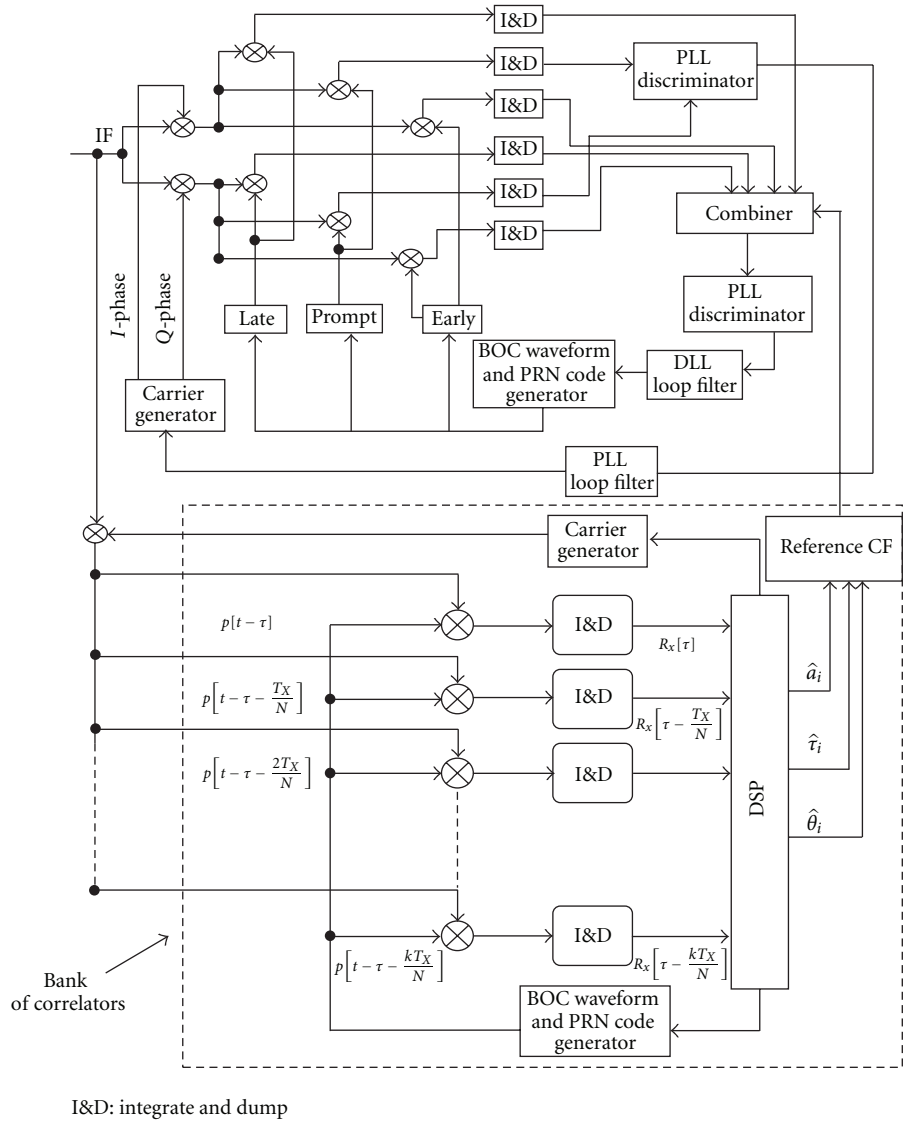

Figure 11: Block diagram of the proposed side peaks cancellation method.

Based on these equations, the MEDLL algorithm can be summarized as follows [21].

Step 1 (Initialization). (1) Calculate the CCF and find its maximum (called peak 1), and its corresponding delay, amplitude and phase.

Step 2 (Successive multipath CFs cancelation). (1) Subtract the contribution of the calculated peak to yield a new approximation of the CF and find the new peak (peak 2) of the residual CF and its corresponding delay, amplitude, and phase.

(2) Subtract the contribution of peak 2 from the resulting CF and find a new estimate of peak 1.

Step 3 (Convergence). (1) Repeat Step 2, until a certain criterion of convergence is met.

The principle of the two versions of the proposed method is shown in the block diagram of Figure 11.

It should be noted that an initialization phase is needed by using the result of the double-delta correlator [15, 22], due to the presence of side peaks in CFs. By this initialization, the MP parameters estimation algorithm converges easily to the correct maximum.

After the estimation of the parameters of all the components of the received signal, several reference CFs, which are delayed and weighted with the estimated parameters, are combined to produce a reference CCF used for side peaks

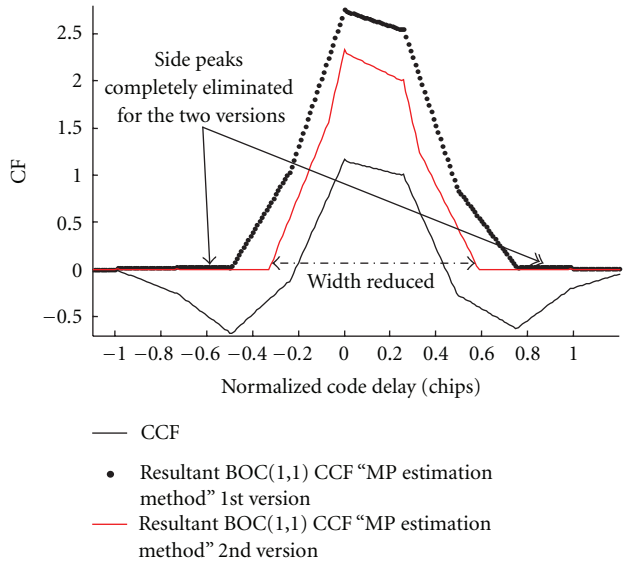

Figure 12: CCF and resultant CCF of BOC(1,1) code after the application of the proposed method (1st and 2nd version with estimation of MP components).

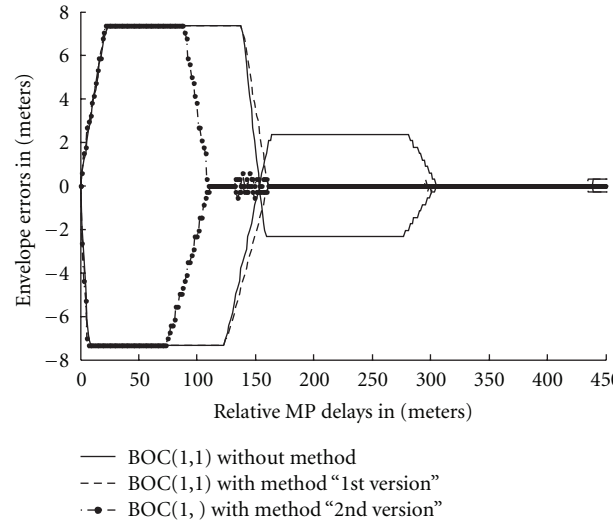

Figure 13: Code error envelopes ($C_s = T_X/10$) of NC and our proposed method for its 1st and 2nd versions (BOC(1,1) code).

cancelation of the received signal CCF. The unambiguous CFs, for the two versions, can be given as follows:

$$R_{\text{Unambiguous}V1}(\tau) = R_{\text{Ambiguous}}(\tau) + \sum_{i=0}^{n} \hat{a}_i \cos\left(\hat{\theta}_i\right) R_{\text{Ideal-PRN}}(\tau - \hat{\tau}_i),$$

$$R_{\text{Unambiguous}V2}(\tau) = R_{\text{Ambiguous}}(\tau) + \sum_{i=0}^{n} \hat{a}_i \cos\left(\hat{\theta}_i\right) \left| R_{\text{Ideal-BOC}}(\tau - \hat{\tau}_i) \right|. \quad (13)$$

The resultants unambiguous CFs, after the application of the proposed method (BOC(1,1) code), are shown in Figure 12.

As shown in this figure, the resulting CCFs from the 1st and 2nd versions of the proposed method does not contain any side peaks. In fact, the widths of the CCFs are completely reduced in the second version compared to what we observe in the 1st version. With the same mechanism, we can get the side peaks cancelation of CBOC and TMBOC CFs in presence of MPs.

4. Simulation Results

Simulations are conducted to test the proposed scheme. For this reason, six scenarios are presented.

In the first scenario, three schemes have been simulated. The first scheme is based on the traditional BOC, the second one is based on our proposed scheme in its first version, and the third scheme is based on our proposed scheme in its second version. Here, we consider an LOS signal and a single MP signal. The 20 MHz band-limited CF is used to estimate the MP error envelopes of BOC(1,1), TMBOC, CBOC, and the two versions of the proposed method. The error envelopes are calculated by determining the zero crossings of the DLLs discriminator outputs as a 0.5 amplitude MP signal is varied in delay from 0 to 450 meters with respect to the LOS signal. The MP error envelopes are calculated at the maximum points when the MP signal is at 0° "in phase" or 180° "out of phase" with respect to the LOS. The results are shown in Figures 13, 14, and 15 for, respectively, BOC(1,1), CBOC, and TMBOC.

As illustrated in these three figures, the error envelopes and their bands of variation are completely reduced in our proposed scheme for all the codes. The error envelopes of our proposed scheme decrease to reach zero for the delay which is greater than approximately 150 meters with respect to the LOS in its first version and approximately 100 meters with respect to the LOS in its second version. This is in contrast to the traditional schemes where the errors decrease to reach zero for the delay which is greater than 293 meters with respect to the LOS. These results show the efficiency of our proposed scheme with respect to that of the traditional BOC(1,1), TMBOC, and CBOC. They also show that the second version is more optimal than the first one.

Another type of performances evaluation is the computation of the running average of the envelope error.

It consists of calculating the absolute envelope values and their cumulative sum with the aim of computing the running average error. The criterion used herein is the same as that used in [27]. The results of running average errors are shown in Figures 16, 17, and 18 for, respectively, BOC(1,1), CBOC, and TMBOC with the first and the second versions of our proposed scheme.

As shown in all these figures, the proposed method presents the overall best performances because it is only sensitive for short and medium MP delays concerning its first

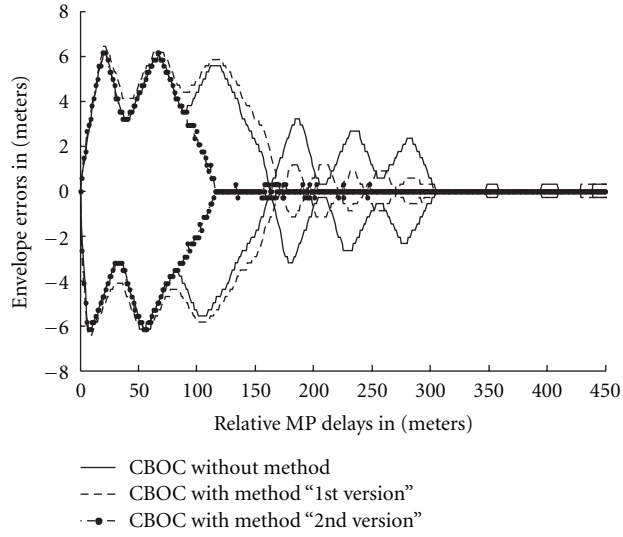

Figure 14: Code error envelopes ($C_s = T_X/10$) of NC and our proposed method for its 1st and 2nd versions (CBOC code).

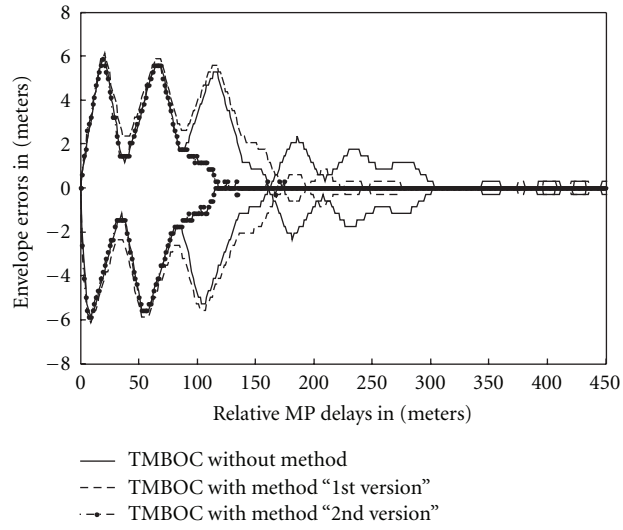

Figure 15: Code error envelopes ($C_s = T_X/10$) of NC and our proposed method for its 1st and 2nd versions (TMBOC code).

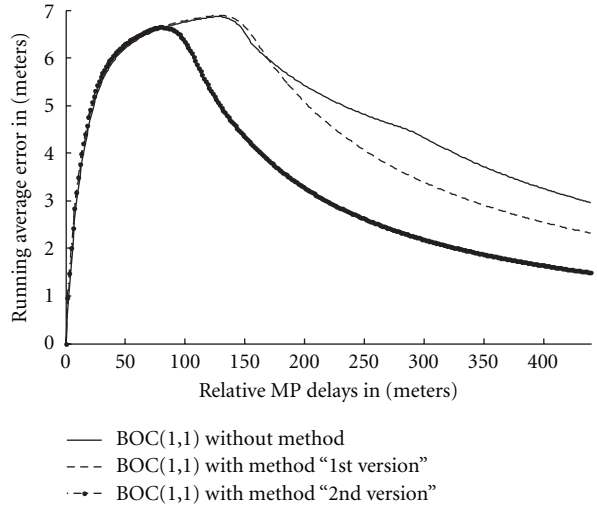

Figure 16: Running average errors ($C_s = T_X/10$) of NC and our proposed method for its 1st and 2nd versions (BOC(1,1) code).

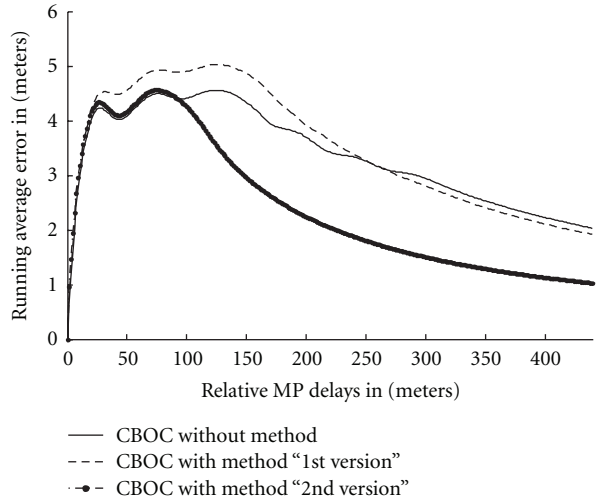

Figure 17: Running average errors ($C_s = T_X/10$) of NC and our proposed method for its 1st and 2nd versions (CBOC code).

version and it is only sensitive for short MP delays concerning its second version.

In the second scenario, all the assumptions of the first scenario are taken into account for comparing our proposed scheme and three other schemes.

In fact, for BOC(1,1) code, four schemes have been simulated: namely, the two versions of our proposed method, the AACF scheme and the SCM scheme. The running average errors are shown in Figure 19.

As illustrated in this figure, our proposed scheme shows the best overall MP performances than that of all other schemes in the sense that it is only sensitive for short MP delays. The running average errors for the two versions decrease rapidly to zero. Also, the band of variation of the bias is less than that of the other schemes. This shows that our proposed scheme has better MP rejection.

For CBOC code, four schemes have been simulated. Both versions of our proposed scheme, the AACF scheme and the PCF scheme for "$x = 1$" in the locally generated code (the authors in [11] assume that the value "$x = 1$" gives the best performances). The running average errors are shown in Figure 20. As shown in this figure, our proposed method in its 2nd version presents the best performances in term of MP rejection and band reduction.

In scenario 3, all the assumptions of the first scenario are also taken into account to compare our proposed scheme in combination with HRC scheme and the traditional BOC(1,1), CBOC, and TMBOC in combination with HRC scheme. The results are shown, through the running average errors, in Figures 21, 22, and 23.

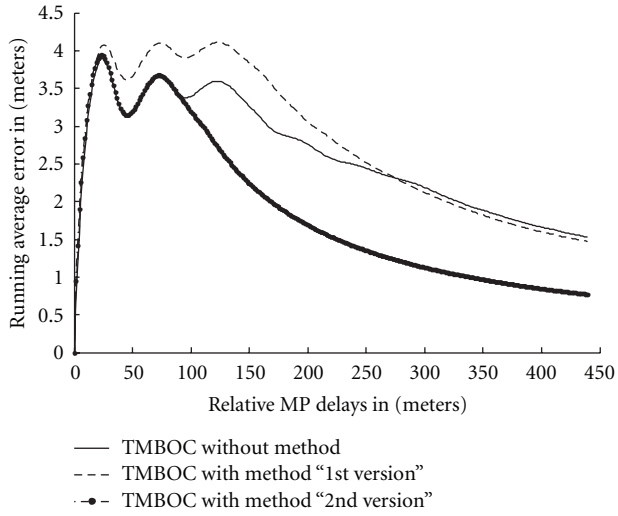

Figure 18: Running average errors ($C_s = T_X/10$) of NC and our proposed method for its 1st and 2nd versions (TMBOC code).

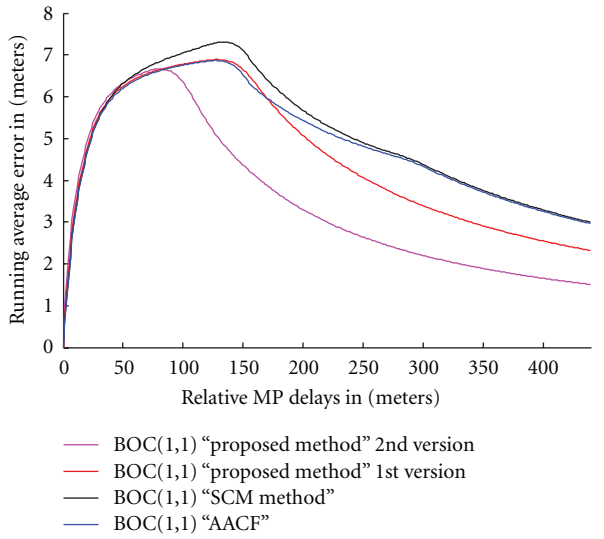

Figure 19: Comparison of running average errors of traditional BOC(1,1), with NC $C_s = T_X/10$, BOC(1,1) with proposed method (1st and 2nd versions), BOC(1,1) with AACF method, and BOC(1,1) with SCM method.

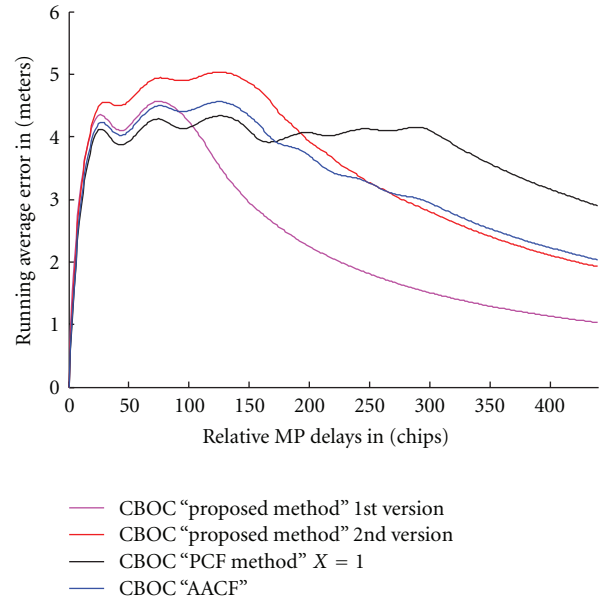

Figure 20: Comparison of running average errors of traditional CBOC with proposed method (1st and 2nd versions), CBOC with AACF method, and CBOC with PCF method.

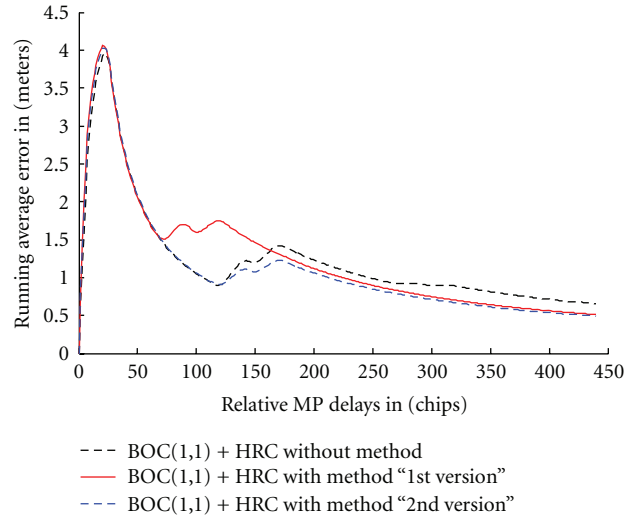

Figure 21: Running average errors of both BOC(1,1)-HRC in combination with our proposed method and BOC(1,1)-HRC without proposed method.

It is clear from all these figures that the performances of our proposed scheme, in combination with HRC scheme, are better than those of the traditional ones in combination with HRC scheme. The running average errors of our proposed scheme (2nd version), in combination with the HRC scheme, decrease rapidly to zero for short MP delays. This proves that our proposed scheme is compatible to the HRC scheme which is originally proposed for MP mitigation in no-BOC signals.

In the scenario four, the proposed unambiguous discriminators are compared with the $\mathrm{BOC}_{\cos}(2,1)$-PRN and $\mathrm{BOC}_{\cos}(6,1)$-PRN with $T_X/2m$ Early-Late Spacing.

Four schemes have been simulated. Both versions of our proposed method (BOC(2,2) and BOC(6,6) codes), $\mathrm{BOC}_{\cos}(2,1)$-PRN discriminator, and $\mathrm{BOC}_{\cos}(6,1)$-PRN discriminator. The MP has an amplitude of 0.5 and its delay is varied from 0 to 1200 meters so that the results can be compared with those of [14]. The precorrelation bandwidth in the receiver and the phases of the MP signal are taken as those of the first scenario. The running average errors are shown in Figure 24.

It can be seen from this figure that our proposed combinations provide good reduction of MP with medium and

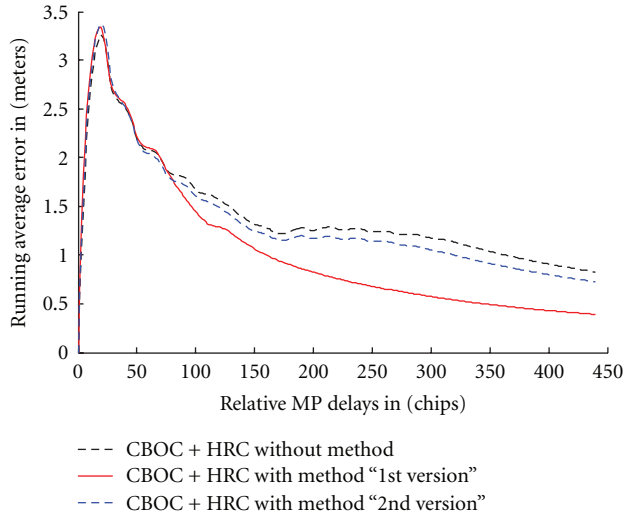

Figure 22: Running average errors of both CBOC-HRC in combination with our proposed method and CBOC-HRC without proposed method.

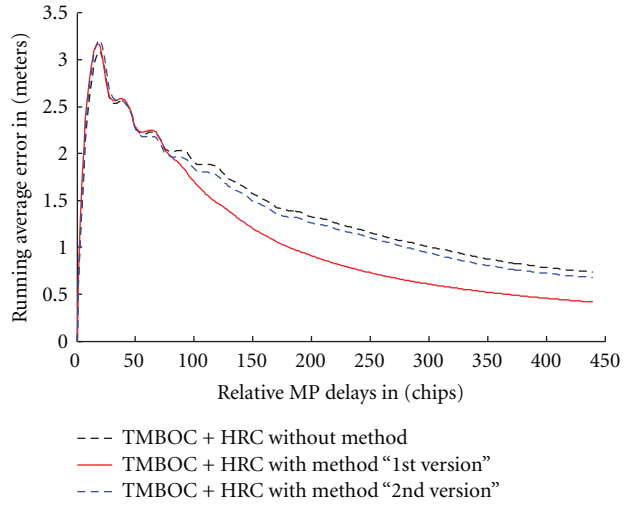

Figure 23: Running average errors of both TMBOC-HRC in combination with our proposed method and TM-HRC without proposed method.

long delay compared to the BOCcos-PRN discriminators. This is due to the sharpest CFs of our proposed method. In addition, our proposed combinations do not present the drawbacks of BOCcos-PRN (due to the flattening of part of the discriminator function [14]) since they exhibit very large linear parts in their discriminator functions.

The scenario five is conducted to test the effect of the signal-to-noise ratio (SNR) on the performances of the proposed method. The results of comparison of the standard deviation (STD) of code tracking for several schemes are shown in Figure 25. Here, we consider the two versions of the proposed method with BOC(n,n) codes ($n = 2$ and $n = 6$), BOCcos(2,1)-PRN method, and BOCcos(2,1)-PRN discriminators. The early late spacing is chosen equal to

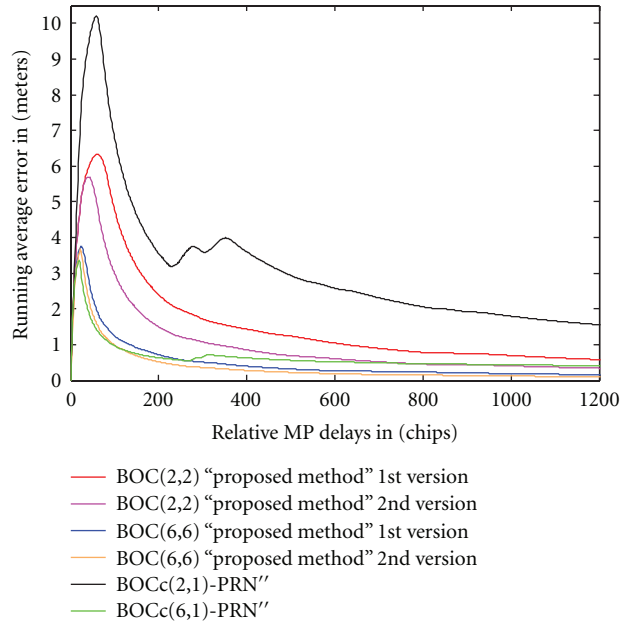

Figure 24: Comparison of running average errors of BOC(2,2), BOC(6,6) (proposed method for its first and second versions), BOCcos(2,1)-PRN and BOCcos(6,1)-PRN.

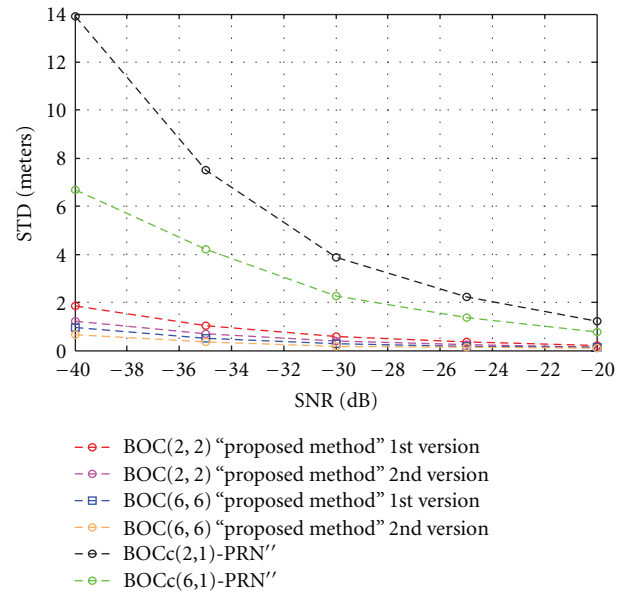

Figure 25: STD of the direct signal delay estimation versus SNR for BOC(2,2), BOC(6,6) (proposed method for its first and second versions), BOCcos(2,1)-PRN, and BOCcos(6,1)-PRN.

$T_X/10$ for our proposed method and $T_X/2m$ for the others schemes.

As illustrated in this figure, the STDs are represented versus SNR which varies from -40 dB to -20 dB. The small STD for the proposed method confirms the applicability of this simplification. In fact, this figure reveals that at low SNR, the proposed method performs better. This could

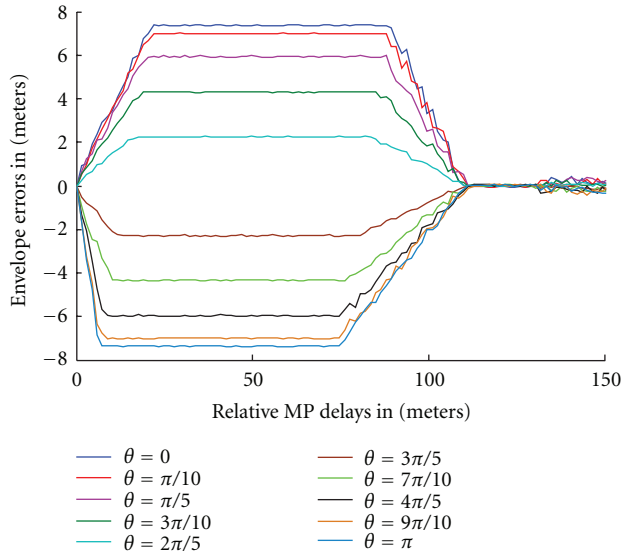

Figure 26: Code error envelopes of BOC(1,1) code with the proposed method (2nd version) for different values of MP phase.

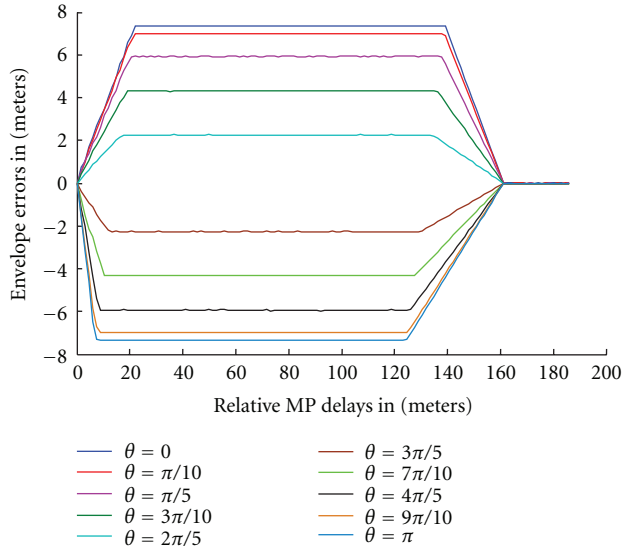

Figure 27: Code error envelopes of BOC(1,1) code with the proposed method (1st version) for different values of MP phase.

be explained by the fact that the $BOC_{cos}(2,1)$-PRN and $BOC_{cos}(6,1)$-PRN bring more noise in the loop.

In the final scenario, we present the envelope errors of our proposed method in its two versions. All the assumptions of the first scenario are also taken into account to examine the applicability of our proposed method for different distortion of MP phase. The phase of the MP is selected in the interval $[0, \pi]$ (with a step of $\pi/10$). The results are shown in Figures 26 and 27 for, respectively, the 1st and 2nd versions.

As illustrated in these two figures, the code error envelopes are similar, in their forms, to those of no-BOC codes. In addition, they are function of the MP phase and they are proportional to the MP phase. This shows the adaptivity and the sensibility of the method to the variation of this distortion.

5. Conclusion

In this paper, an efficient method for side peaks cancelation and MP mitigation in GNSS system is proposed. The scheme, based on the use of reference CFs in combination with the MLE of MP, is shown to completely eliminate the ambiguity problem. Also, it has superior performance on the reduction of the MP error and its band of variation. In addition, it has no special requirements on the finite-bandwidth filter in the receiver due to its sharper CF and it presents a better resistance to the noise. Moreover, it works for both short/long and weak/strong MP. Finally, since the CFs of the proposed method have no side peaks in the CF, all the techniques and methods proposed for MP mitigation in no-BOC signals (such as: traditional GPS code) are practical for our proposed scheme.

References

[1] K. Borre, D. M. Akos, N. Bertelsen, and P. Rinder, *A Software-Defined GPS and Galileo Receiver: A Single-Frequency Approach*, Birkhäauser, Boston, Mass, USA, 2007.

[2] J. W. Betz, "Binary offset carrier modulations for radionavigation," *Navigation, Journal of the Institute of Navigation*, vol. 48, no. 4, pp. 227–246, 2001.

[3] J. A. Avila-Rodriguez, G. W. Hein, S. Wallner et al., "The MBOC modulation: the final touch to the galileo frequency and signal plan," in *Proceedings of the 20th International Technical Meeting of the Satellite Division of The Institute of Navigation (ION GPS '07)*, pp. 1515–1529, Fort Worth, Tex, USA, September 2007.

[4] G. W. Hein, J. A. Avila-Rodriguez, S. Wallner et al., "MBOC: the new optimized spreading modulation recommended for GALILEO L1 OS and GPS L1C," in *Proceedings of the IEEE/ION Position, Location, and Navigation Symposium*, pp. 883–892, San Diego, Calif, USA, April 2006.

[5] F. Bastide, O. Julien, C. Macabiau, and B. Roturier, "Analysis of L5/E5 acquisition, tracking and data demodulation thresholds," in *Proceedings of the US Institute of Navigation GPS*, pp. 2196–2207, Portland, Ore, USA, September 2002.

[6] P. Kovar, F. Vejrazka, L. Seidl, and P. Kacmarick, "Galileo receiver core technologies," *Journal of Global Positioning Systems*, vol. 4, no. 1-2, pp. 176–183, 2005.

[7] A. J. Van Dierendonck, P. Fenton, and T. Ford, "Theory and performance of narrow correlator spacing in a GPS receiver," *Journal of the Institute of Navigation*, vol. 39, no. 3, pp. 265–283, 1992.

[8] O. Julien, C. Macabiau, M. E. Cannon, and G. Lachapelle, "ASPeCT: unambiguous sine-BOC(n,n) acquisition/tracking technique for navigation applications," *IEEE Transactions on Aerospace and Electronic Systems*, vol. 43, no. 1, pp. 150–162, 2007.

[9] A. Burian, E. S. Lohan, and M. K. Renfors, "Efficient delay tracking methods with sidelobes cancellation for BOC-modulated signals," *EURASIP Journal on Wireless Communications and Networking*, vol. 2007, Article ID 072626, 2007.

[10] Y. Zhou, X. Hu, and Z. Tang, "Unambiguous tracking technique for Sin-BOC(1,1) and MBOC(6,1,1/11) signals," in *Proceedings of the 2nd International Conference on Future*

Computer and Communication (ICFCC '10), pp. V1188–V1190, May 2010.

[11] Z. Yao, M. Lu, and Z. Feng, "Unambiguous technique for multiplexed binary offset carrier modulated signals tracking," *IEEE Signal Processing Letters*, vol. 16, no. 7, pp. 608–611, 2009.

[12] F. Dovis, P. Mulassano, and L. Lo Presti, "A novel algorithm for the code tracking of BOC(n,n) modulated signals," in *Proceedings of the 18th International Technical Meeting of the Satellite Division of The Institute of Navigation (ION GNSS '05)*, pp. 152–155, Long Beach, Calif, USA, September 2005.

[13] A. G. Dempster and J. Wu, "Code discriminator for multiplexed binary offset carrier modulated signals," *Electronics Letters*, vol. 44, no. 5, pp. 384–385, 2008.

[14] J. Wu and A. G. Dempster, "Applying a BOC-PRN discriminator to cosine phased BOC(fs, f c) modulation," *Electronics Letters*, vol. 45, no. 13, pp. 689–691, 2009.

[15] G.] McGraw and M. Braasch, "GNSS multipath mitigation using gated and high resolution correlator concept," in *Proceedings of the US ION NTM*, pp. 333–342, San Diego, Calif, USA, January 1999.

[16] M. S. Braasch, "Performance comparison of multipath mitigating receiver architectures," in *Proceedings of the IEEE Aerospace Conference*, vol. 3, pp. 31309–31315, March 2001.

[17] L. Garin et al., "Strobe and edge correlator Mmultipath mitigation for code," in *Proceedings of the 9th Intemational Technical Meeting of the Satellite Division of the Institute of Navigation (ION GPS '96)*, Kansas City, Mo, USA, September 1996.

[18] K. Rouabah, D. Chikouche, F. Bouttout, R. Harba, and P. Ravier, "GPS/galileo multipath mitigation using the first side peak of double delta correlator," *Wireless Personal Communications*, vol. 60, no. 2, pp. 321–333, 2010.

[19] R. D. J. van Nee, J. Siereveld, P. C. Fenton, and B. R. Townsend, "Multipath estimating delay lock loop: approaching theoretical accuracy limits," in *Proceedings of the IEEE Position Location and Navigation Symposium*, pp. 246–251, Las Vegas, Nev, USA, April 1994.

[20] M. Sánchez-Fernández, M. Aguilera-Forero, and A. García-Armada, "Performance analysis and parameter optimization of DLL and MEDLL in fading multipath environments for next generation navigation receivers," *IEEE Transactions on Consumer Electronics*, vol. 53, no. 4, pp. 1302–1308, 2007.

[21] M. Sahmoudi and R. Landry Jr., "Multipath mitigation techniques using maximum-likelihood principle," *Inside GNSS*, vol. 3, no. 8, pp. 24–29, 2008.

[22] M. Sahmoudi and M. G. Amin, "Fast Iterative Maximum-Likelihood Algorithm (FIMLA) for multipath mitigation in the next generation of GNSS receivers," *IEEE Transactions on Wireless Communications*, vol. 7, no. 11, pp. 4362–4374, 2008.

[23] K. Rouabah and D. Chikouche, "GPS/Galileo Multipath detection and mitigation using closed-form solutions," *Mathematical Problems in Engineering*, vol. 2009, Article ID 106870, 20 pages, 2009.

[24] Z. Zhang and C. L. Law, "Short-delay multipath mitigation technique based on virtual multipath," *IEEE Antennas and Wireless Propagation Letters*, vol. 4, no. 1, pp. 344–348, 2005.

[25] Z. Zhang, C. L. Law, and E. Gunawan, "Multipath mitigation technique based on partial autocorrelation function," *Wireless Personal Communications*, vol. 41, no. 1, pp. 145–154, 2007.

[26] F. Dovis, L. L. Presti, M. Fantino, and P. Mulassano, "Comparison between Galileo CBOC Candidates and BOC(1,1) in terms of detection performance," *International Journal of Navigation and Observation*, vol. 2008, Article ID 793868, 9 pages, 2008.

[27] M. Irsigler, J. A. Avila-Rodriguez, and G. W. Hein, "Criteria for GNSS multipath performance assessment," in *Proceedings of the 18th International Technical Meeting of the Satellite Division of The Institute of Navigation (ION GNSS '05)*, pp. 2166–2177, Long Beach, Calif, USA, September 2005.